AGU PUBLICATIONS

Geophysical Research Letters

RESEARCH LETTER
10.1002/2015GL065310

Key Points:
- 1.Amplification of seismic waves at Lusi is sensitive to seismic impedance structure
- 1.Little amplification occurs for our preferred impedance model
- 1.A drilling trigger is more likely than an earthquake trigger

Supporting Information:
- Figures S1–S4

Correspondence to:
M. L. Rudolph,
maxwell.rudolph@pdx.edu

Citation:
Rudolph, M. L., M. Manga, M. Tingay, and R. J. Davies (2015), Influence of seismicity on the Lusi mud eruption, *Geophys. Res. Lett.*, *42*, doi:10.1002/2015GL065310.

Received 9 JUL 2015
Accepted 1 SEP 2015
Accepted article online 3 SEP 2015

Influence of seismicity on the Lusi mud eruption

Maxwell L. Rudolph[1], Michael Manga[2], Mark Tingay[3], and Richard J. Davies[4]

[1]Department of Geology, Portland State University, Portland, Oregon, USA, [2]Department of Earth and Planetary Science, University of California, Berkeley, California, USA, [3]Australian School of Petroleum, University of Adelaide, Adelaide, South Australia, Australia, [4]School of Civil Engineering and Geosciences, University of Newcastle, Newcastle, New South Wales, UK

Abstract Earthquakes trigger the eruption of mud and magmatic volcanoes and influence ongoing eruptive activity. One mechanism that could trigger an eruption is clay liquefaction. Here we model the propagation of seismic waves beneath the Lusi mud eruption (East Java, Indonesia) using available seismic velocity and density models to assess the effect of subsurface structure on the amplification of incident seismic waves. We find that using an updated subsurface density and velocity structure, there is no significant amplification of incident seismic energy in the Upper Kalibeng Formation, the source of the erupting solids. Hence, the hypothesis that the Lusi eruption was triggered by clay liquefaction appears unlikely to be correct. Independent constraints from gas chemistry as well as analyses of drilling activities at the nearby Banjar-Panji 1 gas exploration well and an analysis of the effects of other earthquakes all favor a drilling trigger.

1. Introduction

Earthquakes can trigger magmatic eruptions over subsequent days [*Linde and Sacks*, 1998], with 0.4% of eruptions occurring within a few days of large, regional earthquakes, an eruption frequency that is an order of magnitude greater than the background rate [*Manga and Brodsky*, 2006]. Mud volcano eruptions can similarly be triggered by earthquakes [e.g., *Mellors et al.,* 2007; *Bonini,* 2009], and ongoing eruptions may be influenced by seismicity, with dozens of documented examples [*Manga et al.*, 2009]. Mud volcanoes respond to earthquakes on timescales ranging from hours to months. Immediate or rapid responses to earthquakes are generally attributed to processes controlled by dynamic stresses produced by the passage of seismic waves, while delayed responses may result from processes related to static stress changes.

One high-profile example of a proposed earthquake-triggered eruption is the Lusi mud eruption, East Java, Indonesia. The eruption began on 29 May 2006 and continues today. The erupted mud has displaced approximately 40,000 people and caused economic losses in excess of $4 billion [*Richards,* 2011]. It was proposed that the eruption was triggered by the M_W 6.3 Yogyakarta earthquake [*Mazzini et al.,* 2007, 2009; *Sawolo et al.,* 2009; *Lupi et al.,* 2013, 2014], which struck on 27 May 2006, 2 days prior to the eruption. However, it has also been proposed that the eruption was initiated by drilling operations at gas exploration well Banjar-Panji 1 (BJP-1) located ~200 m from what became the main eruption site [*Manga,* 2007; *Davies et al.,* 2007, 2008; *Tingay et al.,* 2008, 2015]. Although we favor the latter mechanism, owing to the abundance of information about subsurface lithology, structures, fluid chemistry, and physical properties [e.g., *Tingay et al.,* 2015], Lusi provides an ideal test case to explore the mechanisms responsible for short-term triggering of mud volcano eruptions. Owing to the high rate of seismicity in Indonesia, it also provides an opportunity to document how earthquakes influence ongoing eruptions. Here we analyze predicted ground motions at the eruption site, from seismicity before and after the eruption, in order to identify the role of earthquakes in the initiation and modulation of the eruption.

2. Earthquake-Triggering Hypothesis

The hypothesis that the Lusi eruption was triggered by an earthquake was proposed shortly after the eruption began [*Cyranoski,* 2007; *Mazzini et al.,* 2007]. The idea of an earthquake trigger was recently reevaluated by *Lupi et al.* [2013, 2014], who proposed that liquefaction of the mud source in the Upper Kalibeng Formation at approximately 1200–1800 m depth [*Mazzini et al.,* 2007] was induced by the focusing of seismic waves. The focusing was caused by a parabolic seismic reflector whose geometry was inferred from a seismic reflection profile [*Istadi et al.,* 2009], with a change in shear wave velocity (V_S) at a depth of approximately 690 m. The parabolic seismic reflector would focus incident seismic waves into the underlying Upper

Kalibeng shales, liquefying the shales and triggering the eruption. Below 1095 m depth, both V_P and V_S logs are available, but above 1095 m depth, there are no direct measurements of V_S. Depending on the pore pressure at depths above 1095 m, the V_P/V_S ratio could vary rapidly, producing a significant shear wave impedance (the product of density and seismic velocity) contrast. *Lupi et al.* [2014] suggested that a sharp change in pore pressure above the Kalibeng shales, associated with a porosity variation, leads to such a V_S impedance contrast at a depth of approximately 690 m.

The preeruption pore pressure, seismic velocity, and density structure at Lusi were recently reexamined by *Tingay* [2015], who showed that overpressure increased gradually in the clastic sedimentary rocks between 500 and 1100 m depth and that there were no large porosity changes, consistent with overpressures generated by standard disequilibrium compaction processes. Furthermore, the updated petrophysical data set in *Tingay* [2015] indicates that there are no significant shear wave impedance contrasts in the sedimentary rocks overlying the mud source of Lusi and that previously proposed impedance contrasts were based on common artifacts and processing errors in sonic velocity and density data. In this study, we reexamine the earthquake-triggering hypothesis by comparing numerical simulations of seismic wave propagation through each of the proposed seismic velocity structures.

3. Methods

We model 1-D and 2-D seismic wave propagation through a heterogeneous, isotropic medium using a conservative finite difference approach on a fully staggered grid. We use displacement as the dependent variable and calculate stresses and strains at cell centers. The 1-D code uses an eighth-order discretization in space and fourth-order explicit time integration. The 2-D code uses second-order centered differences in both time and space. We performed resolution tests to ensure that numerical dispersion was insignificant for both 1-D and 2-D codes. We benchmarked the codes using synthetic impedance structures to verify the accuracy of transmission and reflection coefficients for plane waves, as well as travel times for layered media. In all calculations, we used a free-surface boundary condition for the surface, and the bottom boundary was placed at a sufficiently great depth (100 km) such that reflections from the bottom boundary did not affect our results. For the 2-D calculations, we used periodic lateral boundary conditions but placed the boundaries sufficiently far from the modeled location of Lusi so that they had no effect on the calculations. As an initial condition, we introduced a single pulse waveform with displacement u described by

$$u(x) = \sin^2(2\pi x/\lambda)$$

where $\lambda = V/\omega$ is the pulse wavelength, V is the velocity of propagation (either V_S or V_P depending on the wave type used for the input motion), ω is the characteristic frequency of the input motion, and x is depth. We consider only vertically incident waves. Due to the very large velocity contrast between the Kalibeng clays and underlying volcanics (Figure 1), we expect incident waves to be strongly refracted toward vertical. We used characteristic input frequencies of 0.25–1 Hz for consistency with previous studies of wave propagation at Lusi [*Lupi et al.*, 2013, 2014] and because these frequencies are known to be effective for triggering mud eruptions [*Rudolph and Manga*, 2012].

In our analyses, we calculate seismic energy density, which has previously been used to define empirical thresholds for earthquake triggering of hydrologic processes including liquefaction, water level changes in wells, and changes in spring and stream flow [e.g., *Wang*, 2007; *Wang and Manga,* 2010]. We define seismic energy density based on kinetic energy (E_k):

$$E_k = \frac{1}{2}\rho v^2$$

as in *Wang* [2007] and *Lay and Wallace* [1995], where ρ is density and v is particle velocity.

We adopt a layered velocity structure with layer geometry either assumed to be planar or distorted using the geometry from *Lupi et al.* [2014] (Figure 1d). The distorted structure is based on a north-south seismic section [*Sawolo et al.,* 2009]. The back azimuth to the Yogyakarta earthquake is ~260°, but east-west structure in an orthogonal seismic section is similar [*Lupi et al.,* 2014]. We use two different velocity and density models to assign layer properties, shown in Figures 1a–1c. First, we use the velocity and density structure model from *Lupi et al.* [2014]. Second, we use the model from *Tingay* [2015]. For each of these velocity models, we

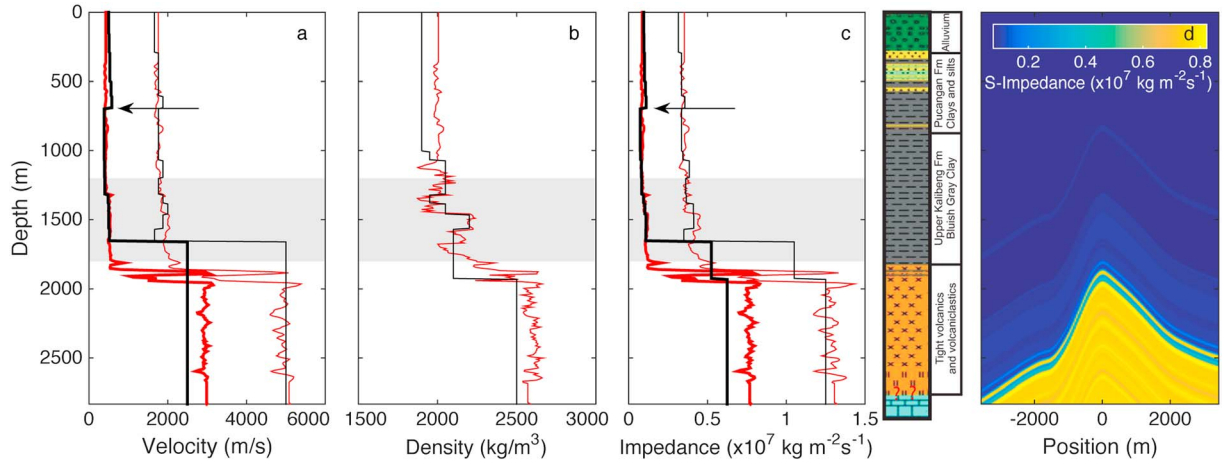

Figure 1. Profiles of seismic velocities and density used in our numerical experiments. In all panels, the black line corresponds to *Lupi et al.* [2014] while red corresponds to *Tingay* [2015]. (a) V_P (thin line) and V_S (bold line), (b) density, and (c) *P* (thin) and *S* (bold) impedance structure for both models. Arrow indicates impedance contrast at approximately 690 m depth in *Lupi et al.* [2014] model. Grey shaded region indicates mud source depth. (d) Example of impedance structure used in 2-D calculations, based on *Lupi et al.* [2014] (horizontal position is specified relative to the apex of the parabolic structure). We also show lithology encountered in BJP-1 between Figures 1c and 1d [*Tingay,* 2015]. All panels share the same vertical axis.

explored cases with and without a distorted structure to separate the effects of impedance contrasts from geometric effects. Throughout the paper, we refer to depths below the surface at the horizontal location of Lusi, which is very close to the apex of the parabolic structure.

4. Results

We illustrate the results of the 1-D wave propagation calculations in Figure 2 and Figures S1–S2 in the supporting information. Figure 2 shows results using $\omega = 0.5$ Hz. Using the *Lupi et al.* [2014] impedance model, maximum seismic energy density over the duration of shaking at a given depth is up to 3 times that for the *Tingay* [2015] model within the Kalibeng clays and the root-mean-square (RMS) seismic energy density is locally up to 90% greater as well.

In Figure 3, we show results from our 2-D wave propagation experiments. Figure 3d shows the RMS seismic energy density from 2-D wave propagation calculations performed using the antiformal structure from

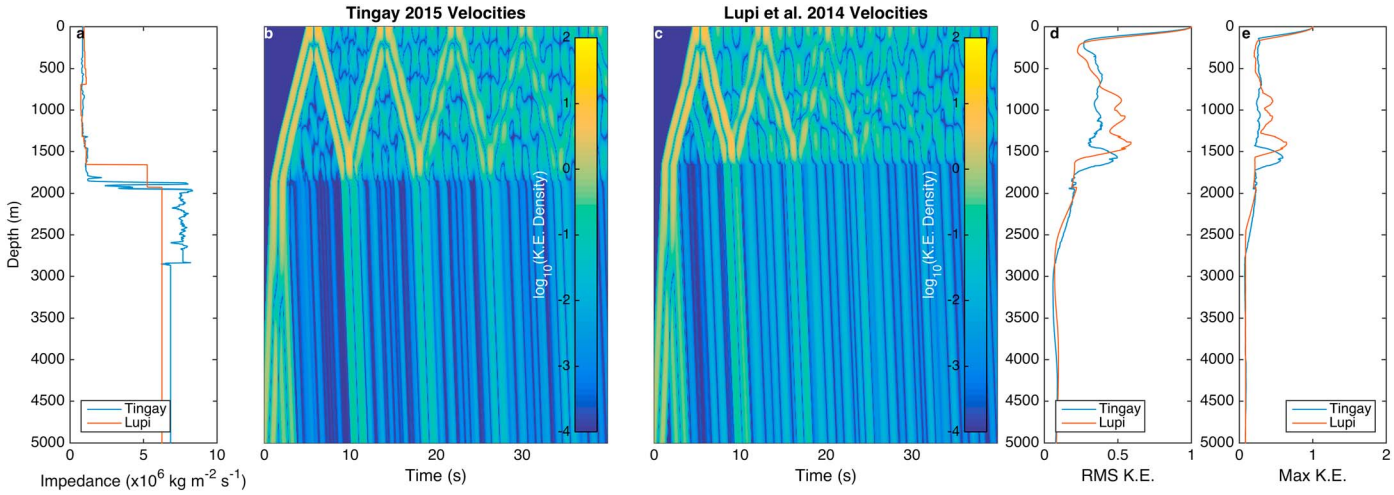

Figure 2. Amplification of ground motion in 1-D calculations for input motion with characteristic frequency $\omega = 0.5$ Hz. (a) Impedance structures used. (b) Kinetic energy density versus depth and time using *Tingay* [2015] velocity model, normalized by kinetic energy density of input waveform. Note that color scale is logarithmic. (c) Same as Figure 2b except using *Lupi et al.* [2014] velocity model. (d) Root-mean-square (RMS) seismic energy density for both models, normalized to equal surface kinetic energy density. (e) Maximum seismic energy density, also normalized to equal surface kinetic energy density.

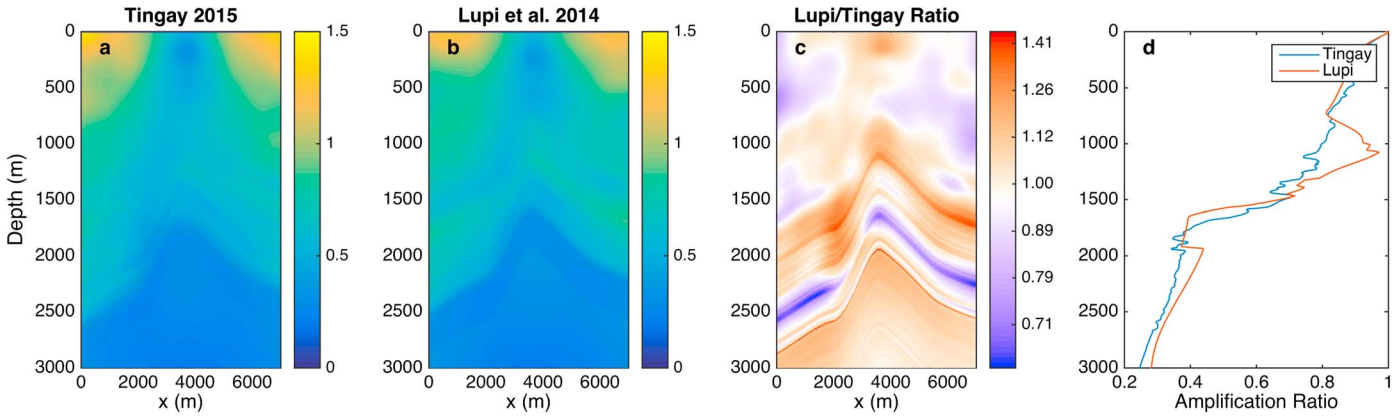

Figure 3. (a) RMS amplification of seismic energy density using *Tingay* [2015] velocity structure in 2-D calculations, normalized by surface RMS seismic energy density, for input motion with $\omega = 0.5$ Hz. Note vertical exaggeration of ~2.3. (b) Same as Figure 3a except using *Lupi et al.* [2014] velocity structure. (c) Ratio of amplifications of seismic energy density in Figures 3a and 3b, with logarithmic color scale. (d) Average of horizontal RMS seismic energy density along the 2-D structure from Figures 3a and 3b, normalized by surface seismic energy density.

Lupi et al. [2013, 2014]. Figure 3 shows the amplification of RMS seismic energy density using the *Lupi et al.* [2014] model relative to the amplification using the *Tingay* [2015] model. Figure 3d shows the average of the amplification ratio from Figure 3c as a function of depth, with the earth structure removed (i.e., depth is calculated relative to the distorted structure). The amplification differs between the two cases shown primarily in the depth range 750–1370 m. In this depth range, the maximum difference in horizontally-averaged amplification between the two velocity models is 24%. We note that while this amplification is less than the 90% found in the 1-D calculations, it is horizontally averaged, and local differences in amplification are much larger. Amplification in the region near the apex of the distorted structure is about 60% greater using the *Lupi et al.* [2014] model than using the *Tingay* [2015] model.

5. Discussion

In layered media, impedance contrasts cause seismic waves to split into transmitted and reflected waves whose amplitudes are controlled by the change in impedance, as well as the angle of incidence of the wave. In our 1-D models, the direction of wave propagation is always normal to the layer interfaces, and thus, the transmitted and reflected wave amplitudes depend only on the impedance structure. The largest impedance contrast in the velocity models occurs at the top of the Plio-Pleistocene volcanics and volcaniclastics, which underlie the Pleistocene Upper Kalibeng clays. This interface appears as a bright reflector in seismic reflection profiles [e.g., *Mazzini et al.,* 2007]. This interface is present at a depth of ~1870 m in the *Tingay* [2015] velocity model, consistent with drilling records, but at a shallower depth of 1657 m in the *Lupi et al.* [2014] model. Because upgoing waves see this contrast as a reduction in impedance, most of the energy is transmitted, and the transmitted wave amplitude is larger than the incident wave amplitude. The second significant impedance contrast exists only for shear waves, and only in the *Lupi et al.* [2014] model at a depth of 690 m (Figure 1); near this depth, *Tingay* [2015] instead has order-of-magnitude smaller velocity contrasts associated with two thin sand layers. There is no apparent reflector at this depth at the BJP-1 location in seismic reflection profiles. When upgoing waves encounter the increase in impedance proposed at this depth by *Lupi et al.* [2014], there is a significant downward reflection of incident energy. This reflection is clearly visible in Figure 2c but absent in Figure 2b (using the *Tingay* [2015] model) and accounts for the differences in maximum and RMS seismic energy density between the calculations between depths of approximately 700–1800 m shown in Figures 2d and 2e. Reflections from the free surface, and from the interface between the volcanics and Pleistocene sediments, have a strong tendency to trap energy in the shallow subsurface. These reflections lead to prolonged shaking in the Pleistocene clastic sedimentary rocks overlying the volcanics.

In our 2-D models, the time history of dynamic strain associated with seismic waves is far more complex, because the angle of incidence across interfaces varies due to the imposed earth structure, and in addition to transmission and reflection, there are conversions between *S* and *P* waves at each layer interface. Nevertheless, the depth-dependent *S* and *P* wave impedance structure still exerts a first-order control on

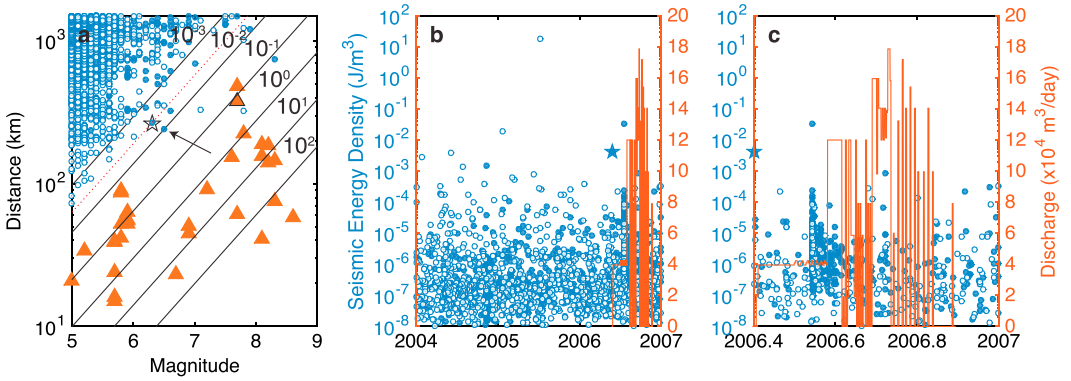

Figure 4. (a) Earthquake magnitude versus epicentral distance for triggered mud volcano eruptions (red triangles) (catalog from *Manga et al.* [2009] and *Rudolph and Manga* [2010, 2012]). Also shown are contours of seismic energy density in J m^{-3}. Blue circles indicate historic seismicity within 1500 km of Lusi (from the USGS catalog) preceding the eruption. Filled and open circles correspond to events shallower and deeper than 30 km, respectively. The event enclosed by the black star is the Yogyakarta earthquake. The event indicated by the black arrow was both larger and closer but did not initiate an eruption. (b) Seismic energy density calculated for earthquakes from USGS catalog preceding Yogyakarta event and discharge from Lusi (digitized from *Mazzini et al.* [2007]). Blue star indicates Yogyakarta earthquake. (c) Same as Figure 4b except showing only the period from 27 May 2006 to 31 December 2006.

amplification of seismic waves, and we see clear differences among the calculations performed with the two velocity structures (Figure 3). As with the 1-D experiments, the introduction of the impedance contrast at 690 m depth in the *Lupi et al.* [2014] model results in significantly greater RMS seismic energy density in the Upper Kalibeng clays.

Our knowledge of the velocity and density structure at Lusi comes from sonic and petrophysical logging of the BJP-1 borehole, with additional independent constraints on compressional velocity from check shot survey data. Because shear wave velocity measurements are only available below the casing shoe at 1095 m depth in BJP-1, there are no direct measurements of V_S at the 690 m depth of the reflector present in the *Lupi et al.* [2014] model. All studies of the velocity structure at Lusi agree that there is no significant variation in the *P* wave velocity above the Upper Kalibeng clays, and geological samples from BJP-1 indicate that there is no significant V_P or V_S contrast in this zone [*Tingay,* 2015]. There is, however, disagreement over the most probable shear wave velocity structure. The V_P/V_S ratio depends on effective stress (lithostatic pressure minus pore pressure), and at low effective stress (near-lithostatic pore pressure), the V_P/V_S ratio can become very large. *Lupi et al.* [2014] argue that there is a significant, abrupt onset of high pore pressures immediately above the Kalibeng clays and that this abrupt variation in pore pressure would modify effective stress, and therefore shear wave velocity. However, the analysis in *Tingay* [2015] of drilling records and petrophysical logs from BJP-1 and nearby (offset) wells shows that pressures are reliably estimated from drilling mud weight in BJP-1 and from six kicks (influxes of fluid into the borehole) and 53 instances of connection gases (gas entering the borehole when segments of the drill string are being connected because drilled mud is temporarily not circulating) or background gas peaks, as well as from offset well measurements. This pore pressure data set demonstrates a shallow onset of overpressure (approximately 350 m) and that effective stress remains nearly constant throughout the entire sedimentary succession overlying the volcanics (0–1870 m depth), as is typical of overpressures generated by common disequilibrium compaction mechanisms. *Tingay* [2015] also used four petroleum industry standard methods for estimating V_S, which all yielded consistent estimates that do not display any significant V_S contrasts. The absence of any major V_S contrasts is in agreement with the lack of V_P contrasts. Global sedimentary rock data sets demonstrate that V_P and V_S are strongly correlated, other than in almost zero effective stress conditions and gas saturated rocks [*Castagna et al.*, 1985; *Lee*, 2010], neither of which are applicable here. In the absence of a shallow shear wave impedance contrast, seismic amplifications are reduced by 70%.

In addition to assessing the local amplitude of ground motion, other observations provide constraints on an earthquake trigger for the Lusi eruption. The M_W 6.3 Yogyakarta earthquake occurred on 27 May 2006, 2 days prior to and 260 km distant from the initial eruption of mud and fluids at Lusi. In Figure 4a, we show historical seismicity within 1500 km of Lusi from the U.S. Geological Survey (USGS) earthquake catalog

(earthquake.usgs.gov). In this magnitude-distance-triggering diagram, we also show known global instances of mud volcano eruptions triggered by earthquakes (compiled in *Manga et al.* [2009] and *Rudolph and Manga* [2010, 2012]). Diagonal lines are contours of constant seismic energy density, and the event indicated with a star is the Yogyakarta earthquake. The USGS earthquake catalog contains 10 prior earthquakes, occurring between 1973 (the beginning of the catalog) and the onset of the mud eruption, for which expected seismic energy densities at Lusi are greater than that calculated for the Yogyakarta earthquake. These events occurred as recently as 2005 and as early as 1976, and none of these triggered an eruption. Of these earthquakes, eight had magnitude greater than the Yogyakarta earthquake and, hence, were more likely to produce a response due to the possible frequency dependence of potential triggering mechanisms [*Manga et al.,* 2009; *Rudolph and Manga*, 2012]. We do not include deep (>100 km) events in this total, as there may be increased sensitivity to shallow earthquakes [*Lupi et al.*, 2013]; Figure 4 distinguishes between deep (>30 km) and shallow earthquakes. While the Yogyakarta event was a strike-slip earthquake, the fault orientation and azimuth to Lusi were such that directivity effects would not have enhanced ground motion at Lusi [*Walter et al.,* 2008]. There was nothing obviously distinctive about the Yogyakarta earthquake relative to other events preceding the eruption.

The maximum dynamic shear stresses produced by the Yogyakarta earthquake were ~0.1 MPa [*Lupi et al.,* 2013] and perhaps lower considering the calculations and velocity model uncertainties presented here (Figures 2 and 3). This stress change is also small compared to the minimum 2.4 MPa effective normal stress reduction caused by a drilling kick, 18 h before the eruption but 25 h after the earthquake [*Davies et al.,* 2007; *Tingay et al.,* 2008, 2015]. H_2S was detected in the fluids released during the kick [*Tingay et al.*, 2015]. The only known source of H_2S in the East Java Basin is the Miocene carbonates thought to be pierced by the wellbore at approximately 2833 m depth [*Davies et al.*, 2007]. Thus, based on the composition of gases released during the kick and immediately preceding the eruption, there is compelling evidence that the initial erupted fluids contained a significant contribution from a source deeper than the Kalibeng clays. The eruption may have been initiated by this deep fluid release, via the BJP-1 borehole, rather than liquefaction of the shallower Kalibeng clays [*Tingay et al.,* 2015], where ground motion has been hypothesized to be amplified [*Lupi et al.*, 2013]. Independent geophysical evidence from ground deformation [*Rudolph et al.*, 2013] and models of this data indicate that there was a significant subsurface volume change attributed to a deep fluid source (>3000 m depth) [*Shirzaei et al.,* 2015] and is consistent with isotopic analysis of erupted gases at Lusi indicating a potential deep hydrothermal fluid source [*Mazzini et al.*, 2012].

Due to the high level of seismicity in Indonesia, Lusi provides an excellent opportunity to study how earthquakes modulate ongoing eruptions. Ongoing eruptions may be more sensitive to earthquakes than quiescent systems or new eruptions [*Manga et al.,* 2009]. In fact, the Yogyakarta earthquake increased heat discharge or the frequency of small pyroclastic flows at nearby active magmatic volcanoes [*Harris and Ripepe*, 2007; *Walter et al.,* 2007]. In Figures 4b and 4c, we show predicted seismic energy densities of all earthquakes in the USGS catalog for the period 2004–2007, where the blue star indicates the Yogyakarta earthquake. Also shown for reference is the discharge from Lusi in middle to late 2006, digitized from Figure 5 of *Mazzini et al.* [2007]. We note that the discharge data may have large uncertainties and are also subject to nonuniform sampling in both space and time. *Mazzini et al.* [2007] suggested that discharge may have been affected by local seismicity, at least for short periods of time. Figures 4b and 4c shows that there is no clear relationship between measured discharge and seismicity. In particular, the nearby event and aftershock sequence (approximately 2006.5 in Figure 4c) produced no immediate change in discharge despite having estimated seismic energy density exceeding that due to the Yogyakarta event. This indicates that long-term variations in discharge were probably not controlled primarily by seismicity, though there may be short-lived changes in eruption style and intensity not simply captured by discharge measurements [*Mazzini et al.,* 2007]. The effort to better understand the relationship between seismicity and eruptive activity at Lusi as well as amplification of ground motion would greatly benefit from improved seismic station coverage.

6. Conclusions

Assessing ground motions is a starting point for understanding possible earthquake triggering of mud and magmatic eruptions. We modeled seismic wave propagation through two different subsurface structures to assess the extent to which the mechanical properties of the subsurface contribute to enhanced energy

dissipation in the Upper Kalibeng Formation, the source of the erupting mud. We found that the amplitude of the seismic energy density in the Kalibeng clays is smaller when using the updated velocity and density structure from *Tingay* [2015] than that produced in otherwise identical calculations using the velocity and density structure from *Lupi et al.* [2014]. The key difference between the two subsurface velocity and density models used is the presence of a shallow (approximately 690 m depth) shear wave impedance contrast in the *Lupi et al.* [2014] model that reflects incident seismic waves downward into the Kalibeng clays. The most thorough published study of pore pressure, petrophysical properties, and subsurface geology does not support the existence of this impedance contrast [*Tingay*, 2015]. Independent constraints on fluid sources from gas geochemistry [*Tingay et al.*, 2015] and surface deformation [*Shirzaei et al.*, 2015] indicate that there was a significant contribution of fluids during the initial phase of the eruption from depths greater than that of the Kalibeng clays. The contribution of fluids from deeper sources indicates that any potential earthquake-triggering processes must have occurred much deeper than the source of the erupting solids, and where there is no obvious reason for ground motion to be amplified. In summary, we find nothing in the earthquake response to disfavor an eruption triggered by the blowout of BJP-1 [e.g., *Davies et al.*, 2007; *Tingay et al.*, 2015]. Owing to the large amount of geochemical, geological, and geophysical data about subsurface properties, Lusi is well suited to study how eruptions initiate and evolve. Lusi thus remains a fascinating natural laboratory in which to study hydrothermal and eruptive processes and social impacts [e.g., *Richards*, 2011] and to test models for longevity [*Davies et al.,* 2011; *Rudolph et al.*, 2011, 2013].

Acknowledgments

We thank Matteo Lupi for providing us with the material properties used in *Lupi et al.* [2013] in MATLAB format and Chi-Yuen Wang for helpful discussion and comments. All data required to reproduce the results shown here are available by request from the corresponding author. This work was partially supported by NSF award EAR-1344424. We thank the Editor Andy Newman and two anonymous reviewers whose comments improved the manuscript.

The Editor thanks two anonymous reviewers for their assistance evaluating this paper.

References

Bonini, M. (2009), Mud volcano eruptions and earthquakes in the Northern Apennines and Sicily, Italy, *Tectonophysics*, *474*(3–4), 723–735, doi:10.1016/j.tecto.2009.05.018.

Castagna, J. P., M. L. Batzle, and R. L. Eastwood (1985), Relationships between compressional-wave and shear wave velocities in clastic silicate rocks, *Geophysics*, *50*, 571–581, doi:10.1190/1.1441933.

Cyranoski, D. (2007), Indonesian eruption: Muddy waters, *Nature*, *445*(7130), 812–815, doi:10.1038/445812a.

Davies, R. J., R. E. Swarbrick, R. J. Evans, and M. Huuse (2007), Birth of a mud volcano: East Java, 29 May 2006, *Geol. Soc. Am.*, *17*(2), 4–9.

Davies, R. J., M. Brumm, M. Manga, R. Rubiandini, R. Swarbrick, and M. Tingay (2008), The East Java mud volcano (2006 to present): An earthquake or drilling trigger?, *Earth Planet. Sci. Lett.*, *272*(3), 627–638, doi:10.1016/j.epsl.2008.05.029.

Davies, R. J., S. A. Mathias, R. E. Swarbrick, and M. J. Tingay (2011), Probabilistic longevity estimate for the LUSI mud volcano, East Java, *J. Geol. Soc.*, *168*(2), 517–523, doi:10.1144/0016-76492010-129.

Harris, A. J. L., and M. Ripepe (2007), Regional earthquake as a trigger for enhanced volcanic activity: Evidence from MODIS thermal data, *Geophys. Res. Lett.*, *34*, L02304, doi:10.1029/2006GL028251.

Istadi, B., G. Pramono, and P. Sumintadireja (2009), Modeling study of growth and potential geohazard for LUSI mud volcano: East Java, Indonesia, *Mar. Pet. Geol.*, *26*, 1724–1739.

Lay, T., and T. C. Wallace (1995), *Modern Global Seismology*, Academic Press, London, U. K.

Lee, M. W. (2010), Predicting S-wave velocities for unconsolidated sediments at low effective pressure, U.S. Geological Survey Scientific Investigations Report 2010–5138.

Linde, A. T., and I. S. Sacks (1998), Triggering of volcanic eruptions, *Nature*, *395*(6705), 888–890, doi:10.1038/27650.

Lupi, M., E. H. Saenger, F. Fuchs, and S. A. Miller (2013), Lusi mud eruption triggered by geometric focusing of seismic waves, *Nat. Geosci.*, *6*(8), 642–646.

Lupi, M., E. H. Saenger, F. Fuchs, and S. A. Miller (2014), Corrigendum: Lusi mud eruption triggered by geometric focusing of seismic waves, *Nat. Geosci.*, *7*(9), 687–688, doi:10.1038/ngeo2239.

Manga, M. (2007), Did an earthquake trigger the May 2006 eruption of the Lusi Mud volcano?, *Eos Trans. AGU*, *88*(18), 201, doi:10.1029/2007EO180009.

Manga, M., and E. Brodsky (2006), Seismic triggering of eruptions in the far field: Volcanoes and geysers, *Annu. Rev. Earth Planet. Sci.*, *34*, 263–291, doi:10.1146/annurev.earth.34.031405.125125.

Manga, M., M. Brumm, and M. L. Rudolph (2009), Earthquake triggering of mud volcanoes, *Mar. Pet. Geol.*, *26*(9), 1785–1798.

Mazzini, A., H. Svensen, G. Akhmanov, G. Aloisi, S. Planke, A. Malthe-Sørenssen, and B. Istadi (2007), Triggering and dynamic evolution of Lusi mud volcano, Indonesia, *Earth Planet. Sci. Lett.*, *261*, 375–388.

Mazzini, A., A. Nermoen, M. Krotkiewski, Y. Podladchikov, S. Planke, and H. Svensen (2009), Strike-slip faulting as a trigger mechanism for overpressure release through piercement structures. Implications for the Lusi mud volcano, Indonesia, *Mar. Pet. Geol.*, *26*(9), 1751–1765, doi:10.1016/j.marpetgeo.2009.03.001.

Mazzini, A., G. Etiope, and H. Svensen (2012), A new hydrothermal scenario for the 2006 Lusi eruption, Indonesia. Insights from gas geochemistry, *Earth Planet. Sci. Lett.*, *317–318*, 305–318, doi:10.1016/j.epsl.2011.11.016.

Mellors, R., D. Kilb, A. Aliyev, A. Gasanov, and G. Yetirmishli (2007), Correlations between earthquakes and large mud volcano eruptions, *J. Geophys. Res.*, *112*, B04304, doi:10.1029/2006JB004489.

Richards, J. R. (2011), Report into the past, present, and future social impacts of Lumpur Sidoarjo, Humanitus Sidoarjo Fund.

Rudolph, M. L., and M. Manga (2010), Mud volcano response to the 4 April 2010 El Mayor-Cucapah earthquake, *J. Geophys. Res.*, *115*, B12211, doi:10.1029/2010JB007737.

Rudolph, M. L., and M. Manga (2012), Frequency dependence of mud volcano response to earthquakes, *Geophys. Res. Lett.*, *39*, L14303, doi:10.1029/2012GL052383.

Rudolph, M. L., L. Karlstrom, and M. Manga (2011), A prediction of the longevity of the Lusi mud eruption, Indonesia, *Earth Planet. Sci. Lett.*, *308*(1–2), 124–130, doi:10.1016/j.epsl.2011.05.037.

Rudolph, M. L., M. Shirzaei, M. Manga, and Y. Fukushima (2013), Evolution and future of the Lusi mud eruption inferred from ground deformation, *Geophys. Res. Lett.*, *40*, 1089–1092, doi:10.1002/grl.50189.

Sawolo, N., E. Sutriono, B. P. Istadi, and A. B. Darmoyo (2009), The LUSI mud volcano triggering controversy: Was it caused by drilling?, *Mar. Pet. Geol.*, *26*(9), 1766–1784, doi:10.1016/j.marpetgeo.2009.04.002.

Shirzaei, M., M. L. Rudolph, and M. Manga (2015), Deep and shallow sources for the Lusi mud eruption revealed by surface deformation, *Geophys. Res. Lett.*, *42*, 5274–5281, doi:10.1002/2015GL064576.

Tingay, M. (2015), Initial pore pressures under the Lusi mud volcano, Indonesia, *Interpretation*, *3*(1), SE33–SE49, doi:10.1190/INT-2014-0092.1.

Tingay, M., O. Heidbach, R. Davies, and R. Swarbrick (2008), Triggering of the Lusi mud eruption: Earthquake versus drilling initiation, *Geology*, *36*(8), 639–642, doi:10.1130/G24697A.1.

Tingay, M., M. L. Rudolph, M. Manga, R. J. Davies, and C.-Y. Wang (2015), Initiation of the Lusi mudflow disaster, *Nat. Geosci.*, doi:10.1038/ngeo2472.

Walter, T. R., R. Wang, M. Zimmer, H. Grosser, B. Lühr, and A. Ratdomopurbo (2007), Volcanic activity influenced by tectonic earthquakes: Static and dynamic stress triggering at Mt. Merapi, *Geophys. Res. Lett.*, *34*, L05304, doi:10.1029/2006GL028710.

Walter, T. R., et al. (2008), The 26 May 2006 magnitude 6.4 Yogyakarta earthquake south of Mt. Merapi volcano: Did lahar deposits amplify ground shaking and thus lead to the disaster?, *Geochem. Geophys. Geosyst.*, *9*, Q05006, doi:10.1029/2007GC001810.

Wang, C.-Y. (2007), Liquefaction beyond the near field, *Seismol. Res. Lett.*, *78*(5), 512–517, doi:10.1785/gssrl.78.5.512.

Wang, C.-Y., and M. Manga (2010), Hydrologic responses to earthquakes and a general metric, *Geofluids*, *10*(1–2), 206–216.